18. Fujisawa, H. *et al.* Thermal diffusivity of Mg_2SiO_4, Fe_2SiO_4, and NaCl at high pressures and temperatures. *J. Geophys. Res.* **73,** 4727–4733 (1968).
19. Schatz, J. F. & Simmons, G. Thermal conductivity of earth materials at high temperatures. *J. Geophys. Res.* **77,** 6966–6983 (1972).
20. Katsura, T. Thermal diffusivity of olivine under upper mantle conditions. *Geophys. J. Int.* **122,** 63–69 (1995).
21. Shankland, T. J., Nitsan, U. & Duba, A. G. Optical absorption and radiative heat transport in olivine at high temperature. *J. Geophys. Res.* **84,** 1603–1610 (1979).
22. Murase, T. & McBirney, A. R. Properties of some common igneous rocks and their melts at high temperatures. *Bull. Geol. Soc. Am.* **84,** 3563–3592 (1973).
23. Büttner, R., Zimanowski, B., Blumm, J. & Hagemann, L. Thermal conductivity of a volcanic rock material (olivine-melilitite) in the temperature range between 288 and 1470 K. *J. Volcanol. Geotherm. Res.* **80,** 293–302 (1998).
24. Shore, M. Comment on "Experimental determination of the thermal conductivity of molten $CaMgSi_2O_6$ and the transport of heat through magmas". *J. Geophys. Res.* **100,** 22401–22402 (1995).
25. Tiller, W. A. *The Science of Crystallization: Macroscopic Phenomena and Defect Generation* (Cambridge Univ. Press, 1991).
26. Cockayne, B., Chesswas, M. & Gasson, D. B. Facetting and optical perfection in Czochralski grown garnets and rubies. *J. Mater. Sci.* **4,** 450–456 (1969).
27. Brandon, S. & Derby, J. J. Heat transfer in vertical Bridgman growth of oxides: effects of conduction, convection, and internal radiation. *J. Cryst. Growth* **121,** 473–494 (1992).
28. Tsukada, T., Kakinoki, K. & Hozawa, M. Effect of internal radiation within crystal and melt on Czochralski crystal growth of oxide. *Int. J. Heat Mass Transfer* **38,** 2707–2714 (1995).
29. Chai, M., Brown, J. M. & Slutsky, L. J. Thermal diffusivity of mantle minerals. *Phys. Chem. Miner.* **23,** 470–475 (1996).
30. Burns, R. G. *Mineralogical Applications of Crystal Field Theory* 2nd edn (Cambridge Univ. Press, 1993).
31. Donaldson, C. H. Laboratory duplication of comb layering in the Rhum pluton. *Mineral. Mag.* **41,** 323–336 (1977).

Acknowledgements. We thank A. M. Hofmeister for comments on the manuscript. This work was supported by NSERC.

Correspondence and requests for materials should be addressed to A.D.F. (e-mail: afowler@uottawa.ca).

A ferric-chelate reductase for iron uptake from soils

Nigel J. Robinson*, Catherine M. Procter*, Erin L. Connolly† & Mary Lou Guerinot†

* *Department of Biochemistry and Genetics, The Medical School, University of Newcastle, Newcastle NE2 4HH, UK*
† *Department of Biological Sciences, Dartmouth College, Hanover, New Hampshire 03755-3576, USA*

Iron deficiency afflicts more than three billion people worldwide[1], and plants are the principal source of iron in most diets. Low availability of iron often limits plant growth because iron forms insoluble ferric oxides, leaving only a small, organically complexed fraction in soil solutions[2]. The enzyme ferric-chelate reductase is required for most plants to acquire soluble iron. Here we report the isolation of the *FRO2* gene, which is expressed in iron-deficient roots of *Arabidopsis*. FRO2 belongs to a superfamily of flavocytochromes that transport electrons across membranes. It possesses intramembranous binding sites for haem and cytoplasmic binding sites for nucleotide cofactors that donate and transfer electrons. We show that *FRO2* is allelic to the *frd1* mutations that impair the activity of ferric-chelate reductase[3]. There is a nonsense mutation within the first exon of *FRO2* in *frd1-1* and a missense mutation within *FRO2* in *frd1-3*. Introduction of functional *FRO2* complements the *frd1-1* phenotype in transgenic plants. The isolation of *FRO2* has implications for the generation of crops with improved nutritional quality and increased growth in iron-deficient soils.

Arabidopsis is an 'iron-efficient' plant, able to acquire iron from soils of low iron availability, but the genetic basis of iron efficiency is unclear. In such plants, the activity of ferric-chelate reductase at the plasma membrane of root epidermal cells increases when iron is deficient[4,5]. Organic compounds of either plant or microbial origin that retain Fe^{3+} in the soil solution have a lesser affinity for Fe^{2+}. It is therefore likely that ferric-chelate reductase activity releases iron from organic compounds, generating free iron for uptake[6]. Because the ferric-chelate reductase of plant roots has some functional similarity to the human phagocytic NADPH oxidase gp91phox (ref. 7) and yeast ferric-chelate reductases such as FRE1 (ref. 8) and FRP1 (ref. 9), we speculated that it may share elements of structural similarity with these enzymes. The enzymes are involved in the transfer of electrons from cytosolic donors to FAD and then, through two consecutive haem groups, to single electron acceptors on the opposing face of a membrane. The haem groups are coordinated to four conserved histidine residues located on two transmembrane α-helices[10]. However, gp91phox and the yeast ferric-chelate reductases have in common only a few short sequence motifs, most notably associated with the cofactor-binding sites.

Two approaches were initiated to obtain a ferric-chelate reductase gene: generating reductase-deficient plant mutants[3], and cloning candidate plant DNA sequences. Degenerate oligonucleotide primers were designed to anneal to sequences encoding the only tetrapeptide motif (the FAD-binding site) common to gp91phox and the yeast ferric-chelate reductases, and to a second partly conserved motif associated with the NADPH-binding sites. Several polymerase chain reaction (PCR) products were amplified from *Arabidopsis* genomic DNA using a low annealing temperature. Seven products were cloned and sequenced and one, which encodes a serine-rich polypeptide, was selected for further analysis because FRP1 is serine rich in the region between the cofactor-binding sites. This PCR product was used to screen genomic and complementary DNA libraries, and a genomic fragment containing two closely related genes, designated *FRO1* and *FRO2*, was fully sequenced (Fig. 1a). The *FRO2* intron–exon boundaries were identified from the cDNA sequence; the *FRO1* intron–exon boundaries were deduced by analogy to *FRO2* by using predictions[11] of 5′ donor and 3′ acceptor sites and by reverse transcriptase PCR (RT-PCR). FRO2 and FRO1 have 61.9% sequence identity (90.5% similarity). Flanking the 3′ end of *FRO1* is a synvergently transcribed gene encoding a cytochrome P450, designated *CYP86A4* (Fig. 1a), followed by a convergently transcribed unknown gene with similarity to the expressed sequence tags Z17619, N96903 and H76348. Flanking the 5′ end of *FRO2* is a synvergently transcribed gene related to *MKP4* that encodes a deduced mitogen-activated protein (MAP) kinase (not shown on Fig. 1a).

The sequence and predicted structure of FRO2 is shown in Fig.1, FRO2 is composed of 725 amino acids, has a predicted pI of 9.37 and relative molecular mass (M_r) of 81.50, although the presence of glycosylation motifs suggest that the native protein may have a greater M_r. FRO2 contains sequences identical to the FAD-binding site and the conserved region adjacent to the NADPH-binding site of FRE1 (underlined in Fig. 1b) but no other identical sequence motifs of an equivalent length. However, predictions of secondary structure indicate further similarity. The amino-terminal regions of the yeast ferric-chelate reductases and gp91phox form several transmembrane α-helices that are apparent in hydrophobicity plots. Six hydrophobic domains are identified within the N-terminal regions of FRO2 along with two carboxy-terminal hydrophobic domains, all of which are predicted[12] to form transmembrane α-helices. This suggests that an intracellular region of FRO2, containing the deduced cofactor-binding sites, is anchored at both ends by membrane-spanning regions (Fig. 1c). In contrast, the gp91phox and yeast ferric-chelate reductase cofactor-binding sites and associated C-terminal regions are all predicted to be cytosolic. To form an active complex, gp91phox requires a second membrane protein, p22phox. The total number of predicted transmembrane α-helices in FRO2 is equivalent to the number in gp91phox (six) and p22phox (two) combined, and it is feasible that the C-terminal domain, including the two additional transmembrane α-helices in FRO2, performs an analogous function to p22phox (p22phox shows 10% identity and 50% sequence similarity to the C-terminal domain of FRO2). Two pairs of histidine residues in FRO2 that lie on two predicted, similarly orientated, transmembrane α-helices are in equivalent locations (Fig. 1b) to the histidine residues in FRE1 and gp91phox that coordinate haem[10] (Fig. 1c).

Arabidopsis frd1 mutants do not induce ferric-chelate reductase activity, so they do not translocate ^{55}Fe to shoots when roots are presented with $^{55}Fe^{3+}$-chelates[3]. The *frd1* mutations map towards the top of chromosome 1, 0 centiMorgans from markers PVV4 (ATHACS) and 19 centiMorgans from NCCl (ref. 3). Partial DNA sequences from the ends of the bacterial artificial chromosome clones F9C19 and T1617 (GenBank accession numbers B11604 and B09869, respectively) show identity to sections of the MAP kinase gene and *CYP86A4* that flank *FRO2* and *FRO1*. F9C19 and T1617 cross-hybridize with the yeast artificial chromosome clones yUP20D1, yUP12D7 and CIC3H3, which contain sequences that also map near to PVV4 (ref. 13). These data indicate that the region shown in Fig. 1a is located on chromosome 1 at, or close to, the *frd1* mutations. Sequencing both cDNA and genomic DNA from allelic mutants *frd1-1* and *frd1-3* revealed non-synonymous nucleotide substitutions within *FRO2*: a nonsense mutation in the first exon of *frd1-1* and the substitution of a threonine codon with a methionine codon in *frd1-3* (Fig. 2a). The amino-acid substitution in *frd1-3* lies within the deduced tetrapeptide FAD-binding site. Relative to the wild type, *frd1-1* mutants had impaired growth on media with no added iron (Fig. 2b) but equivalent growth on media supplemented with 100 μM Fe^{3+} EDTA (Fig. 2c).

We generated transgenic *frd1-1* plants that carry a genomic DNA fragment including *FRO2* and 0.6 kilobase (kb) of sequence 5′ of the *FRO2* ATG start codon. Low-iron-inducible root-surface ferric-chelate reductase activity was restored in these plants (Fig. 3), confirming that the *frd1* phenotypes are brought about by the observed mutations in *FRO2*. An equivalent restoration of ferric-chelate reductase activity was observed in three independent transformed lines.

Semiquantitative RT-PCR reveals that *FRO2* transcripts are more abundant than *FRO1* transcripts in roots (data not shown) and that *FRO2* transcripts accumulate in response to iron deficiency (Fig. 4a). This suggests that increased ferric-chelate reductase activity under these conditions involves the synthesis of the enzyme, rather than merely the activation of pre-existing reductase. The amount of *FRO2* transcript is reduced in *frd1-1* and increased in *frd1-3* (Fig. 4b). Premature termination of translation of *FRO2* in *frd1-1*

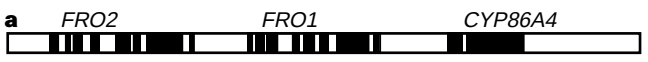

b

```
FRE1 MVRTRVLFCLFISFFATVQSSATLISTSCISQAALYQFGCSSKSKSCYCK

FRO2        MEIEKSNNGGSNPSAGEEFKDMIKGVTKFLMMVIFLGTIMLWI
FRE1 NINWLGSVTACAYENSKSNKTLDSALMKLASQCSSIKVYTLEDMKNIYLN

FRO2 MMPTLTYRTKWLPHLRIKFGTSTYFGATGTTLFMYMFPMMVVACLGCVYL
FRE1 ASNYLRAPEKSDKKTVVSQPLMANETAYHYYYEENYGIHLNLMRSQWCAW

FRO2 HFKNRKSPHHIDRETKGGVWSKLRKPMLVKGPLGIVSVTEITFLAMFVAL
FRE1 GLVFFWVAVLTAATILNILKRVFGKNIMANSVKKSLIYPSVYKDYNERTF
FRP1 MAINSSDKWTVIAICLILGILLAFILMFWLERFRVIIKSNAHKHDPSDKR

FRO2 LLWCFITYLRNSFATITPKSA----------------------AAHDES
FRE1 YLWKRLPFNFTTRGKGLVVLIFVILTILSLS-FGHNIKLP-----HPYDR
FRP1 QIWLEKYYLFVRQIYTYLVTHKVILTLIAVIPVVAISIPFIGMQTPASSH
gp91 ------MGNWAVNEGLSIFVILVWLGLNVFLFVWYYRVYDIPPKFF----

FRO2 LWQAKLESAALRLGLIGNICLAFLFL-----------PVARGSSLLPAMG
FRE1 PRWRRSMAFVSRRADLMAIAL-F-------PVV-YLFGIRNNPFIPITGL
FRP1 GKQTTQVSTGNWSKNAVAARLGFLACGLYVTSY--FFSIKNNPFALLLIS
gp91 YTRKLLGS-ALALARAPAACLNFNCMLILLPVCRNLLSFLRGSSACCSTR
                          L F
FRO2 LTSESSIKY--HIWLGHMVMALFTVHGLCYIIYWASMHEISQMIMWD---
FRE1 SFSTFNFY---HKWSAYVCFMLAVVHSIVMTASGVKRGVFQSLVRK----
FRP1 SHEKMNYV---HRRLSQYAIMIGAIHGFAYIG-LAAQGKRALLTAR----
gp91 VRRQLDRNLTFHKMVAWMIALHSAIHTIAHLFNVEWCVNARVNNSDPYSV
               H              H
FRO2 -----------TKGVSNLAGEIALAAGLVMWATTYPK-------------
FRE1 -------------FYFRWGIVATILMSIIIFQSEKV---------------
FRP1 ----------------VTI-IGYVILGLMVIMIV-----------------
gp91 ALSELGDRQNESYLNFARKRIKNPEGGLYLAVTLLAGITGVVITLCLILI

FRO2 -------IRRRFFEVFFYTHYLY-IVFMLFFVLHVGIS-FSFIALPGFYI
FRE1 -------FRNRGYEIFLLIHKAMNIMFIIAMYYHCHTLGWMGWIWSMAGI
FRP1 --SSLPFFRRRFYEWFFVLHHMCSIGFLITIWLH-HRR-CVVYMKVCVAV
gp91 ITSSTKTIRRSYFEVFWYTHHLFVI-FFIGLAIHGAERIVRGQTAESLAV
           R    E F   H    I F      H
FRO2 FLVDRFLRFLQSRENVRLLAARILPSDTMELTFSKNSKLVYSPTSI----
FRE1 LCFDRFCRIVRIIMNGGLKTATLSTTDDSNVIKISVKKPKFFKYQVGAFA
FRP1 YVFDRGCRMLRSFLNR-SKFDVVLVEDDLIYMKGPRPKKSFFGLPWGAGN
gp91 HNITVCEQKISEWGKIKECPIPQFAGNPPMTWKWIVGPMFLYLCERLVRF

FRO2 ----MFVNIPSIS--------------------------------KLQWH
FRE1 YMYFL-----SPKSAW----------------------------FYSFQSH
FRP1 H---MYINIPS------------------------------LSYWQIH
gp91 WRSQQKVVITKVVTHPFKTIELQMKKKGFKMEVGQYIFVKCPKVSKLEWH
                                                    H
```

```
FRO2 PFTITS-SSKLEPE-KLSIVIKKEGKWSTKLHQRLSSSDQIDRL------
FRE1 PFTVLSERHRDPNNPDQLTMYVKANKGITRVLLSKVLSAPNHTV------
FRP1 PFTIASVPSDDFIELFVAVRAGFTKRLAKKVS-SKSLSDVSDINISDEKI
gp91 PFTLTSAPEED--FFSIHIRIV--GDWTEGLFNACGCDKQEFQDAW----
     PFT  S
FRO2 -------------------------------AVSVEGPYGPASADFLRHEA
FRE1 ----------------------------DCKIFLEGPYGVTVPHIAKLKR
FRP1 EKNGDVGIEVMERHSLSQEDLVFESSAAKVSVLMDGPYGPVSNPYKDYS-
gp91 --------------------------KLPKIAVDGPFGTASEDVFSYEV
                                      GP G
FRO2 --LVMVCGGSGITPFISVIRDLIATSQKETCKIPKITLICAFKKSSEISM
FRE1 N-LVGVAAGLGVAAIYP--HFVECLRLPSTDQLQHK---FYWIVNDLSHL
FRP1 -YLFLFAGGVGVSYILP--IILDTIKKQS-RTV-HIT--FVWSAR-SSAL
gp91 VMLVG-AGI-GVTPFASILKSVWYKYCNNATNLKLKKIYFYWLCRDTHAF
       L       G
FRO2 LDLVLPLSGLETELSSDINIKIEAFITRDNDAG----------DE-----
FRE1 KWFENELQWLKE-----KSCEVSVIYTGSSVEDTNSDESTKGFDDKE---
FRP1 LNIVHKSLCEAVR-----YTEMNINIFCHLTNSYP----VEEVSSLNSQS
gp91 EWFADLLQLLESQMQERNAGFLSYNIYLTGWDESQANHFAVHHDEEKDV-

FRO2 AKAGKIKTLWFKPSLSDQSISSILGPNSWLWL-GAILASSFLIFMIIIGI
FRE1 ESEITVECLNKRPDLKELVRSEIKLSELENNNITFYSCGPATFNDDFRNA
FRP1 ARNYSLQYLNGRPDVNDYFKDFLHATGTQT--AALASCGSDKLLRHLKSC
gp91 ITGLKQKTLYGRP--NWDNEFKTIASQHPNTRIGVFLCGPEALAETLSKQ
               L   P
FRO2 ITRYYIYPIDHNTNKIYSLTSKTIIYILVISVSIMATCSAAMLWNKKKYG
FRE1 VVQGIDSSLKIDVELEEEESFTW
FRP1 VNTHSPSTVDLYQHYEEI
gp91 SISNSESGPRGVHFIFNKENF

FRO2 KVESKQVQNVDRPSPTSSPTSSWGYNSLREIESTPQESLVQRTNLHFGER

FRO2 PNLKKLLLDVEGSSVGVLVCGPKKMRQKVAEICSSGLAENLHFESISFSW
```

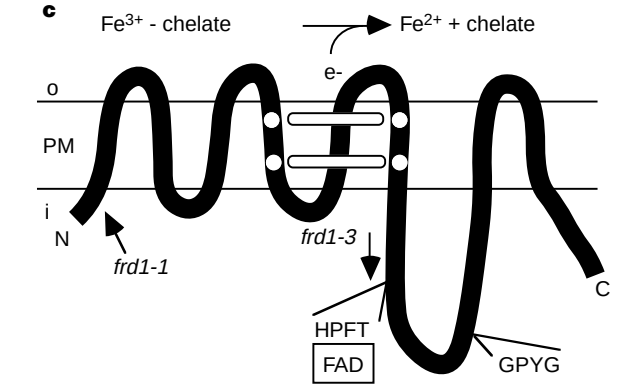

Figure 1 The sequence and predicted structure of FRO2. **a**, Genomic organization of *FRO2*, *FRO1* and *CYP86A4* within 15.2 kb of contiguous sequence. Black boxes represent exons. **b**, The deduced sequence of FRO2 aligned with FRE1, FRP1 and gp91phox (gp91) with residues showing identity to FRO2 in bold and two motifs associated with cofactor binding underlined. The FRO2 sequence presumes initiation at the first transcribed, in-frame start codon. **c**, Hypothetical plasma membrane (PM)-associated structure of FRO2. Four histidine residues (white spots) predicted to coordinate two intramembraneous haem groups (white bars) are indicated; i, inside cell; o, outside cell.

might be expected to reduce transcript stability and hence abundance. Accumulation of non-functional FRO2 in *frd1-3* may impair any feedback inhibition of transcription.

Iron uptake by leaf mesophyll cells seems to involve the action of a plasma-membrane ferric-chelate reductase, which is presumed to release the metal from ligands in the translocation stream[14]. Relatively little is known about the transport of iron in phloem or its uptake by developing seeds, although changes in iron demand in aerial tissues alters the activity of root-surface ferric-chelate reductase[15]. In addition to *FRO2* and *FRO1*, we have identified at least three other *FRO* genes in *Arabidopsis*, the products of which may act in different organs or specialized cell types to mediate the translocation of iron[16]. In response to iron deficiency in *Arabidopsis*, there is also increased root-surface copper-chelate reductase activity[3]. Low-iron-inducible copper-chelate reduction is absent in *frd1-1* mutants[3] and is restored in transgenic plants containing *FRO2* (data not shown). However, FRO2-mediated copper reduction may be gratuitous because copper accumulation was not reduced in *frd1* mutants grown on plates[3]; alternatively, it may increase uptake only under certain soil conditions. Furthermore, *FRO2* transcript abundance under iron deficiency was unaffected by exposure to 0.5 μM $CuSO_4$, whereas the addition of 300 μM bathocuproinedisulphonic acid (a copper chelator) further reduced, rather than increased, *FRO2* transcript abundance in plants grown under high-iron conditions for 3 days (data not shown). Some *FRE1* and *FRE2* homologues of the yeast *Saccharomyces cerevisiae* are regulated by the iron-responsive transcription factor AFT1, and some are regulated by the copper-responsive transcription factor MAC1 (ref. 17). Other FRO proteins may also be produced in response to low levels of copper.

We also identified an expressed sequence tag from rice with sequence similarity to gp91phox, and the corresponding gene, *rbohA*, was subsequently sequenced[18]. Homologues of *rbohA* have now been identified in *Arabidopsis* but their functions remain unclear[19,20]. The deduced Rboh proteins show greater sequence identity than FRO to gp91phox, with sequence trees placing the FRO proteins in a clade separate from the Rboh proteins and gp91phox. Plants resist pathogens by means of the swift, localized production of O_2^- and H_2O_2, which is reminiscent of the oxidative burst mediated by the gp91phox complex of human phagocytic

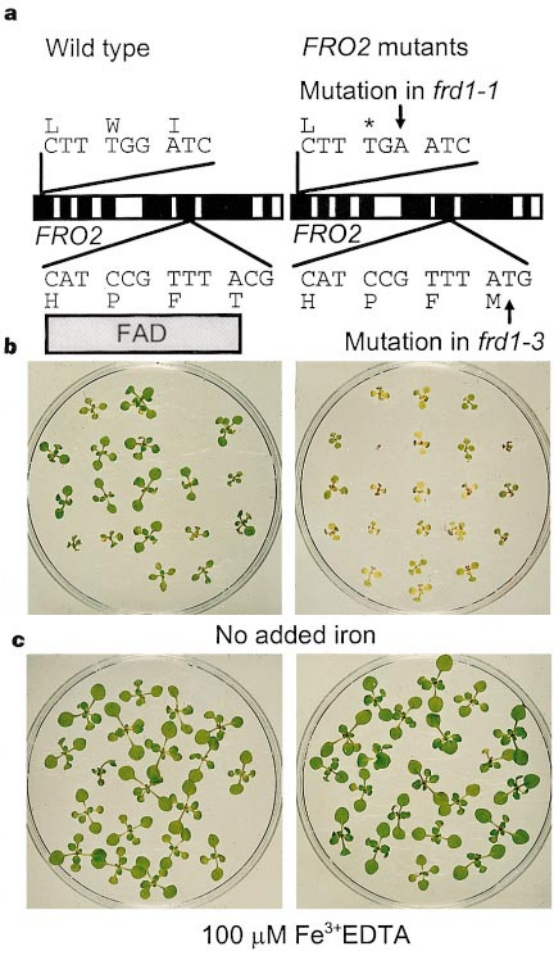

Figure 2 *FRO2* mutations in ferric-chelate reductase-deficient *frd1 Arabidopsis* and the influence of iron on growth. **a**, Schematic representation of the *FRO2* gene (black boxes represent exons) and mutations in the first exon of *FRO2* in *frd1-1* and within the region encoding the predicted FAD-binding site in *frd1-3*. **b**, Growth of wild-type (Columbia Col-0) (left) and *frd1-1* mutants (right) for 14 days on Gamborg's agar plates containing no micronutrient iron. **c**, Growth of wild-type (Columbia Col-0) (left) and *frd1-1* (right) for 14 days on Gamborg's agar plates containing 100 μM Fe^{3+} EDTA.

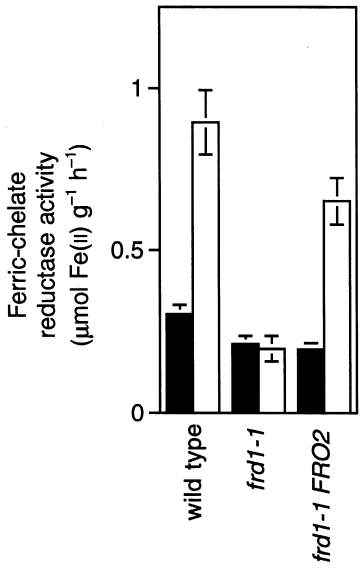

Figure 3 Assays of ferric-chelate reductase activity in wild type (Columbia *gl1*), *frd1-1* mutants and transgenic *frd1-1* mutants containing *FRO2*, showing that *FRO2* complements the *frd1* mutant phenotype. Values are mean of ten assays of ferric-chelate reductase activity in plants grown in the presence (black columns) or absence (white columns) of added Fe^{3+} EDTA using previously described conditions[3].

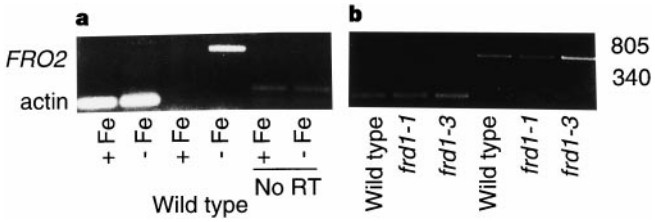

Figure 4 Semiquantitative RT-PCR showing *FRO2* transcript abundance in roots. **a**, Effects of iron (+Fe or –Fe) on transcript abundance in wild-type *Arabidopsis* (Columbia Col-0). Actin (lanes 1, 2) and *FRO2* (lanes 3, 4) amplification products are of the anticipated sizes for cDNA. A control reaction containing no reverse transcriptase (lanes 5, 6) generated a trace amount of product (faint band) of the (slightly larger) size anticipated from genomic DNA template using the actin primers. **b**, Transcript abundance under –Fe conditions in wild-type (Columbia C24) and *frd1* mutant plants using actin (lanes 1–3) and *FRO2* (lanes 4–6) primers.

neutrophil membranes. It has therefore been suggested that the products of the *rboh* genes act to generate reactive oxygen species for defence against plant pathogens[18–20]. Data showing that at least one member (FRO2) of this superfamily of proteins is engaged in the transfer of electrons across a plant cell membrane to a single electron acceptor support the proposal that the Rboh proteins function in a similar manner but donate electrons to different acceptors.

The isolation of the *FRO* gene family has revealed a biochemical mechanism for ferric-chelate reduction by plants. We are now able to investigate the contributions of different reductase enzymes in the acquisition of exogenous iron and the distribution of iron between different cell types and organs. These genes may also be used as markers in selective breeding programmes or may be manipulated in transgenic plants to generate higher-yielding, iron-efficient or iron-rich crops. To improve human iron nutrition, it will not be sufficient merely to increase iron uptake by plants but modified uptake and/or translocation is likely to be a contributory factor. □

Methods

Gene isolation and characterization. Degenerate primers 5′-(C/T)(G/T)I (G/C)A(A/G)(A/T)II CA(C/T)CCI TT(C/T) AC-3′ and 5′-IIC C(A/G)(A/T) AIG GIC CIT C-3′ (where I represents deoxyinosine, and alternative deoxynucleotides at a single position are shown in parentheses) were designed to anneal to sequences encoding residues [L/F/W][Q/E][W/I/S]HPFT and [D/E]GP[Y/F]G corresponding to conserved motifs in FRE1, FRE2 (ref. 21), FRP1 and gp91phox. Genomic DNA from *Arabidopsis* (Ler) was used as template for 30 cycles of PCR with *Taq* DNA polymerase and standard buffer conditions but with 7 mM $MgCl_2$ and 1 μM of each primer; annealing, extension, denaturing were at 35 °C (2 min), 72 °C (1 min), 92 °C (1 min), respectively, and products were resolved on a 2% agarose gel. Seven different DNA fragments were cloned and sequenced. A probe prepared by random primer labelling[22] of the insert (172 base pairs) in one of these clones (designated J1) was used to screen a mixed-tissue *Arabidopsis* cDNA library[23] by standard protocols[24], and one hybridizing partial cDNA (1.4 kb) was identified from 800,000 plaques. A plasmid containing the cDNA was recovered in *Escherichia coli* strain DH10B[ZIP] (Gibco BRL), the insert was sequenced and found to share 85% identity at the nucleotide level with the original PCR product, and the corresponding gene was subsequently designated *FRO3*. A probe was generated using the *FRO3* cDNA fragment and used to screen an *Arabidopsis* (Ler) genomic library[25] in λFIX (Stratagene). Six hybridizing clones were isolated from 200,000 plaques. Restriction mapping showed that they belonged to two groups with three clones containing the 3′-end of *FRO3*. The other three genomic clones contained various spans of another genomic region. The entire sequence of one of these genomic clones and part of another were determined to generate 15.2 kb of continuous sequence. This genomic region contains two related genes in tandem, designated *FRO2* and *FRO1*. The original PCR product, J1, was found to be identical to a section of *FRO1*. A full-length *FRO2* cDNA was subsequently obtained by screening a cDNA library prepared from RNA isolated from roots[26].

Semiquantitative RT-PCR. Wild-type *Columbia* (Col-0 and its variant C24) and mutant *Arabidopsis* were grown for 14 days on Gamborg's agar containing 100 μM Fe^{3+} EDTA, followed by 3 days on either no added iron but with 300 μM ferrozine (-Fe), or 100 μM Fe^{3+} EDTA (+Fe). For analysis of the effects of copper, plants were grown for the final 3 days on minimal medium agar containing no added iron either with or without 0.5 μM $CuSO_4$; some plants were grown for a final 6 days on minimal medium agar, with or without 300 μM bathocuproinedisulphonic acid (a copper chelator); 100 μM Fe^{3+} EDTA was added to both media for the final 3 days. Total RNA was extracted from excised roots using TRI-Reagent (Sigma), and 2 μg was used to synthesize cDNA with a dT_{15} oligonucleotide and M-MLV reverse transcriptase (Gibco BRL). PCR with cDNA was performed using standard conditions with primers (5′-GAG ATA GAA ATC CTG AGA GG-3′ and 5′-CAA AGA CCA TGA ACG GTG-3′) designed to anneal to *FRO2* in preference to other *FRO* genes. Amplification of actin cDNA was used as an internal control in comparative RT-PCR experiments with primers (5′-GGT AAC ATT GTG CTC AGT GGT GG-3′ and 5′-CTC GGC CTT GGA GAT CCA CAT C-3′) designed to anneal to any of the ten known *Arabidopsis* actin genes[27].

Plant transformation and assay of ferric-chelate and copper-chelate reductase. The 6.2-kb *Xba*I genomic fragment from qnrλJ1Z4 (EMBL Y09581), containing the entire *FRO2* coding region and 0.6 kb of upstream sequence, was cloned into the *Xba*I site of pCGN1547 (ref. 28) to yield pELC203, which was used to transform *Agrobacterium tumefaciens* strain ASE to gentamycin resistance[29]. *frd1-1* plants were grown in soil under low light conditions (50–60 $\mu E\,m^{-2}\,s^{-1}$) in preparation for transformation by vacuum infiltration[30]. Transformed plants were identified by selection on kanamycin. Ferric-chelate and copper-chelate reductase activities were assayed in wild-type Columbia *gl1*, *frd1-1* and the transformants, as described previously[3] with the exception that plants were assayed for ferric-chelate reductase activity after four days of growth on iron-deficient or iron-sufficient media.

Received 16 October 1998; accepted 4 January 1999.

1. World Health Organisation ⟨http://www.who.int/nut/malnutrition_worldwide.htm#ida⟩, 25 January 1999.
2. Guerinot, M. L. & Yi, Y. Iron: nutritious, noxious and not readily available. *Plant Physiol.* **104,** 815–820 (1994).
3. Yi, Y. & Guerinot, M. L. Genetic evidence that induction of root Fe(III) chelate reductase activity is necessary for iron uptake under iron deficiency. *Plant J.* **10,** 835–844 (1996).
4. Chaney, R. L., Brown, J. C. & Tiffin, L. O. Obligatory reduction of ferric chelates in iron uptake by soybeans. *Plant Physiol.* **50,** 208–213 (1972).
5. Bienfait, H. F. Regulated redox processes at the plasmalemma of plant root cells and their function in iron uptake. *J. Bioenerg. Biomembr.* **17,** 73–83 (1985).
6. Eide, D. in *Metal Ions in Gene Regulation* (eds Silver, S. & Walden, W.) 342–371 (Chapman and Hall, New York, 1998).
7. Chanock, S. J., Elbenna, J., Smith, R. M. & Babior, B. M. The respiratory burst oxidase. *J. Biol. Chem.* **269,** 24519–24522 (1994).
8. Dancis, A., Klausner, R. D., Hinnebusch, A. G. & Barriocanal, J. G. Genetic evidence that ferric reductase is required for iron uptake in *Saccharomyces cerevisiae*. *Mol. Cell. Biol.* **10,** 2294–2301 (1990).
9. Roman, D. G., Dancis, A., Anderson, G. J. & Klausner, R. D. The fission yeast ferric reductase gene *frp1*$^+$ is required for ferric iron uptake and is homologous to the gp91-phox subunit of the human NADPH phagocyte oxidoreductase. *Mol. Cell. Biol.* **13,** 4342–4350 (1993).
10. Finegold, A. A., Shatwell, K. P., Segal, A. W., Klausner, R. D. & Dancis, A. Intramembrane bis-heme motif for trans-membrane electron transport conserved in a yeast iron reductase and the human NADPH oxidase. *J. Biol. Chem.* **271,** 31021–31024 (1996).
11. Solovyev, V. V., Salamov, A. A. & Lawrence, C. B. Predicting internal exons by oligonucleotide composition and discriminant analysis of spliceable open reading frames. *Nucleic Acids Res.* **22,** 5156–5163 (1994).
12. Milpetz, F., Argos, P. & Persson, B. TMAP- a new email and www service for membrane-protein structural predictions. *Trends Biochem. Sci.* **20,** 204–205 (1995).
13. *Arabidopsis thaliana* Genome Center ⟨http://genome.bio.upenn.edu/physical-mapping/ch1_pt1.html⟩, 25 January 1999.
14. Brüggeman, W., Mass-Kantel, K. & Moog, P. R. Iron uptake in mesophyll cells: the role of plasma membrane bound ferric-chelate reductases. *Planta* **190,** 151–155 (1993).
15. Grusak, M. A. & Pezeshgi, S. Shoot-to-root signal transmission regulates root Fe(III) reductase activity in the *dgl* mutant of pea. *Plant Physiol.* **110,** 329–334 (1996).
16. Robinson, N. J., Sadjuga & Groom, Q. J. The *froh* gene family from *Arabidopsis thaliana*: putative iron-chelate reductases. *Plant Soil* **196,** 245–248 (1997).
17. Martins, L. J., Jensen, L. T., Simons, J. R., Keller, G. L. & Winge, D. R. Metalloregulation of *FRE1* and *FRE2* homologs in *Saccharomyces cerevisiae*. *J. Biol. Chem.* **273,** 23716–23721 (1998).
18. Groom, Q. J. *et al. rbohA*, a rice homologue of the mammalian gp91-phox respiratory burst oxidase gene. *Plant J.* **10,** 515–522 (1996).
19. Keller, T. *et al.* A plant homolog of the neutrophil NADPH oxidase gp91phox subunit gene encodes a plasma membrane protein with Ca^{2+} binding motifs. *Plant Cell* **10,** 1–13 (1998).
20. Torres, M. A. *et al.* Six *Arabidopsis thaliana* homologues of the human respiratory burst oxidase (gp91phox). *Plant J.* **14,** 365–370 (1998).
21. Georgatsou, E. & Alexandraki, D. Two distinctly regulated genes are required for ferric reduction, the first step of iron uptake in *Saccharomyces cerevisiae*. *Mol. Cell. Biol.* **14,** 3065–3073 (1994).
22. Feinberg, A. P. & Vogelstein, B. A technique for radiolabelling DNA restriction endonuclease fragments to high specific activity. *Anal. Biochem.* **132,** 6–13 (1983).
23. Newman, T. *et al.* Genes galore: a summary of the methods for accessing results from large-scale partial sequencing of anonymous *Arabidopsis* cDNA clones. *Plant Physiol.* **106,** 1241–1255 (1994).
24. Benton, W. D. & Davis, R. W. Screening λgt recombinant clones by hybridisation to single plaques *in situ*. *Science* **196,** 180–182 (1977).
25. Voytas, D. F., Konieczny, A., Cummings, M. P. & Ausubel, F. M. The structure, distribution and evolution of the Ta1 retrotransposable element family of *Arabidopsis thaliana*. *Genetics* **126,** 713–721 (1990).
26. Peterman, T. K. & Goodman, H. M. The glutamine synthetase gene family of *Arabidopsis thaliana*: light-regulation and differential expression in leaves, roots and seeds. *Mol. Gen. Genet.* **230,** 145–154 (1991).
27. McDowell, J. M., Huang, S. R., McKinney, E. C., An, Y. Q. & Meagher, R. B. Structure and evolution of the actin gene family in *Arabidopsis thaliana*. *Genetics* **142,** 587–603 (1996).
28. McBride, K. E. & Summerfelt, K. R. Improved binary vectors for *Agrobacterium*-mediated plant transformation. *Plant Mol. Biol.* **14,** 269–276 (1990).
29. Rogers, S. G., Klee, H. J., Horsch, R. B. & Fraley, R. T. Improved vectors for plant transformation: expression cassette vectors and new selectable markers. *Methods Enzymol.* **253,** 253–277 (1988).
30. Bent, A. F. *et al. RPS2* of *Arabidopsis thaliana*: a leucine-rich repeat class of plant disease resistance genes. *Science* **265,** 1856–1860 (1994).

Acknowledgements. We thank Q. J. Groom, funded by BBSRC (N.J.R.), whose work provided a basis for this study. This work was supported by a BBSRC studentship (C.M.P.) and a grant from the US National Science Foundation (M.L.G.).

Correspondence and requests for materials should be addressed to N.J.R. (requests for *FRO* clones; e-mail: n.j.robinson@ncl.ac.uk) or M.L.G. (*frd1* mutants; e-mail: mary.lou.guerinot@dartmouth.edu). FRO1 and FRO2 sequence has been deposited in the EMBL database (accession number Y09851).